Minimum Localizable Damage for Stochastic Subspace-based Damage Diagnosis

Alexander Mendler, Ambroise Cadoret, Clément Freyssinet, Michael Döhler, Yann Lecieux, Laurent Mevel, Carlos Ventura

Minimum Localizable Damage for Stochastic Subspace-based Damage Diagnosis

Alexander Mendler * Ambroise Cadoret ** Clément Freyssinet ** Michael Döhler *** Yann Lecieux **
Laurent Mevel *** Carlos Ventura *

* *Dept. of Civil Engineering, University of British Columbia, Vancouver BC, V6T 1Z4, Canada*
** *GeM, Université de Nantes, 44000 Nantes, France*
*** *Inria, COSYS/SII, I4S, Univ. Gustave Eiffel, 35042 Rennes, France*

ABSTRACT: This article describes an approach to evaluate the minimum localizable damage for stochastic subspace-based damage diagnosis. Localizability is defined as the sensitivity to small and local damages (detectability), the ability to narrow down the exact damage location (localization resolution) and the test response of undamaged parameters (false localization alarms). For the analysis, damage is defined as a change in model-based design parameters, for example, material constants or cross-sectional values in a finite element model. Subsequently, the parameter changes are linked to changes in the global damage-sensitive features using sensitivity vectors, and inherent uncertainties (due to stochastic loads and measurement noise) are quantified. This way, local structural parameters can be tested for changes using statistical hypothesis tests, such as the general likelihood ratio and the statistical minmax localization test. Due to the numerical conditioning of the damage localization problem, the sensitivity vectors have to be clustered before damage can be localized. Sensitivity clustering corresponds to a substructuring of the finite element model, where the number of clusters (the localization resolution) is a user-defined input parameter. The main results of this paper are mathematical criteria to calculate the damage detectability and the false alarm susceptibility for different localization resolutions. Moreover, an automated substructuring routine is described that finds the optimal substructure arrangement as a compromise between high damage detectability, high localization resolution, and low false alarm susceptibility. For proof of concept, a numerical case study is presented, where the damage localizability is determined and validated for a cable-stayed bridge.

KEY WORDS: Ambient vibrations, statistical test, detectability, localization resolution, false localization alarms

1 INTRODUCTION

Modern societies depend on structural and mechanical systems, such as power plants, bridges, offshore platforms, defence systems, aircraft and spacecraft. Because many of these structures cannot be economically replaced or because they are exposed to natural hazards, monitoring techniques are developed to guarantee a safe operation, even beyond their original life span.

In the context of civil engineering structures, the process of implementing a damage diagnosis strategy is referred to as structural health monitoring (SHM). This process is divided into the operational evaluation of the structure, the observation through permanently installed sensors, the extraction of damage-sensitive features, and the subsequent damage diagnosis [1], which is subdivided into damage detection, localization, quantification, and lifetime prognosis [2]. Damage detection can be performed in an unsupervised learning mode, meaning no vibration data from the damaged structure is available. Damage localization and quantification, on the other hand, either require vibration from the damaged structure for training or a finite element (FE) model of the examined structure.

On one hand, FE models are generally over-parametrized, meaning changes in multiple structural parameters have a similar effect on the data-driven features. So, it is not possible to identify the structural parameter that has changed due to damage. This either makes the damage localization impossible or causes false localization alarms, meaning undamaged components are incorrectly classified as damaged. In the literature, multiple approaches are summarized to overcome this problem, for example, the collinearity index method [3], the column-pivoting method [4], the Gram-Schmidt orthogonalization [5], a recursive approach based on principal component analysis as in [6] or other.

On the other hand, the use of FE models allows one to physically define damage and to focus the damage diagnosis on user-defined structural parameters. Moreover, it is possible to calculate the sensitivity of data-driven features toward model-based parameter changes and to extrapolate knowledge beyond the reference state of the structure. This paper explains how the localizable damage can be quantified in percent of a model-based parameter change (in, for example, material properties or cross-sectional values) before damage actually occurs.

All studies in this paper are performed for the stochastic subspace-based damage diagnosis methods, which are capable of detecting [7] and localizing [8] structural changes based on statistical hypothesis tests. The problem of overparametrization is remedied by combining redundant parameters into parameter clusters [9], where the number of clusters (the localization resolutions) depends on a user-defined input parameter [10]. More recently, a method was published to determine the minimum detectable damage based on vibration data from the undamaged structure and a FE model [11]. In the current paper, the method is extended to damage localization, where the mean test response for damaged and undamaged parameters is predicted. The approach has already been described in the automatic control community [12] but has not been applied to larger civil engineering structures, such as bridges.

The paper is organized as follows: Section 2 recaps the stochastic subspace-based damage localization method. Section 3 introduces three optimization criteria to assess the localizability of damage. In Section 4, the approach is applied to a cable-stayed bridge followed by the conclusions in Section 5.

2 STATISTICAL DAMAGE LOCALIZATION

This section recaps the stochastic subspace-based damage diagnosis method. It is based on the asymptotic local approach to damage detection [13] in combination with the stochastic subspace-based residual vector as a damage-sensitive criterion. The underlying vibration model is assumed to be linear and time-invariant, with white noise excitation and no periodic input signals.

2.1 Damage-sensitive Residual

The damage-sensitive feature is formed in the mathematical subspace of covariance functions. Covariance functions describe the similarity of output signals at different measurement channels. They can be estimated based on output data, which is indicated through the hat symbol:

$$\hat{\mathbf{R}}_i = \frac{1}{N}\sum_{k=1}^{N} \mathbf{y}_{\kappa+i}\mathbf{y}_{\kappa}^T \in \mathbb{R}^{r\times r},$$

where i is the time lag, N is the number of samples in the measurement record and r is the number of channels. By arranging the output covariance estimates in block Hankel format

$$\hat{\boldsymbol{\mathcal{H}}}_{p+1,q} = \begin{bmatrix} \hat{\mathbf{R}}_1 & \hat{\mathbf{R}}_2 & \iddots & \hat{\mathbf{R}}_q \\ \hat{\mathbf{R}}_2 & \hat{\mathbf{R}}_3 & \iddots & \hat{\mathbf{R}}_{q+1} \\ \iddots & \iddots & \iddots & \iddots \\ \hat{\mathbf{R}}_{p+1} & \hat{\mathbf{R}}_{p+2} & \iddots & \hat{\mathbf{R}}_{p+q} \end{bmatrix} \tag{1}$$

a dynamic system with m degrees of freedom can be modelled. The parameters p and q are time lag parameters with $\min(pr, qr) \geq n$ and often $p+1 = q$. After applying a singular value decomposition

$$\hat{\boldsymbol{\mathcal{H}}}_{p+1,q} = \begin{bmatrix}\hat{\mathbf{U}}_1 & \hat{\mathbf{U}}_0\end{bmatrix} \begin{bmatrix}\hat{\mathbf{D}}_1 & \mathbf{0} \\ \mathbf{0} & \hat{\mathbf{D}}_0\end{bmatrix} \begin{bmatrix}\hat{\mathbf{V}}_1^T \\ \hat{\mathbf{V}}_0^T\end{bmatrix},$$

the dynamic system matrices can be retrieved from the column space $\hat{\mathbf{U}}_1 \in \mathbb{R}^{(p+1)r\times n}$ using stochastic system identification [14,15], where $n = 2m$. The null space $\hat{\mathbf{U}}_0$ is orthogonal to the column space $\hat{\mathbf{U}}_1$, so a damage-sensitive residual can be formed by pre-multiplying the left null space to the block Hankel matrix and by vectorizing the residual matrix, using the column-stacking operator $\mathrm{vec}(\cdot)$, so [7]

$$\hat{\boldsymbol{\varepsilon}} = \mathrm{vec}(\hat{\mathbf{U}}_0^T \hat{\boldsymbol{\mathcal{H}}}_{p+1,q}). \tag{2}$$

2.2 Damage Parametrization

For a physical interpretation, damage has to be expressed in terms of model parameters and linked to the damage-sensitive feature using sensitivity analysis. Using FE models, the health state can be expressed through model-based design parameters $\boldsymbol{\theta} \in \mathbb{R}^H$ with (i.e., material properties, cross-sectional values, support conditions, or pre-stressing forces), and damage can be defined as a deviation from their reference values $\boldsymbol{\theta}^0$, so

$$\boldsymbol{\Delta} = \boldsymbol{\theta} - \boldsymbol{\theta}^0. \tag{3}$$

Using a first-order Taylor series expansion, the residual's mean vector can be expressed in terms of the parameter vector as

$$\mathrm{E}_{\boldsymbol{\theta}}[\hat{\boldsymbol{\varepsilon}}] \approx \mathrm{E}_{\boldsymbol{\theta}^0}[\hat{\boldsymbol{\varepsilon}}] + \boldsymbol{\mathcal{J}}(\boldsymbol{\theta} - \boldsymbol{\theta}^0), \tag{4}$$

where the first term approximates a zero vector $\mathrm{E}_{\boldsymbol{\theta}^0}[\hat{\boldsymbol{\varepsilon}}] \to \mathbf{0}$ and the second term includes the Jacobian matrix $\boldsymbol{\mathcal{J}}$, which holds the feature's derivative with respect to structural parameters, that is,

$$\boldsymbol{\mathcal{J}} = \left.\frac{\partial \mathrm{E}_{\boldsymbol{\theta}}[\hat{\boldsymbol{\varepsilon}}]}{\partial \boldsymbol{\theta}}\right|_{\boldsymbol{\theta}=\boldsymbol{\theta}^0}. \tag{5}$$

The Jacobian matrix links changes in the data-driven residual vector to model-based design parameters, which allows for a physical interpretation of changes in data. More information on the analytical computation of the Jacobian matrix for the residual from Eq. (2) can be found in the literature [9,10].

2.3 Statistical Distributions of the Feature

Uncertainties due to stochastic loads, measurement noise, and limited sample size N have to be considered to guarantee a reliable damage diagnosis. It can be shown that the residual vector approximates a multi-dimensional normal distribution

$$\boldsymbol{\zeta} = \sqrt{N}\hat{\boldsymbol{\varepsilon}} \longrightarrow \begin{cases} \mathcal{N}(\mathbf{0}, \boldsymbol{\Sigma}) & \text{(reference)} \\ \mathcal{N}(\boldsymbol{\mathcal{J}}\boldsymbol{\delta}, \boldsymbol{\Sigma}) & \text{(damaged)} \end{cases} \tag{6}$$

where $\boldsymbol{\zeta}$ is known as the Gaussian residual vector and $\boldsymbol{\delta} = \sqrt{N}(\boldsymbol{\theta} - \boldsymbol{\theta}^0)$ is the asymptotic change vector, cf. Eq. (4). Damage manifests itself in a changing parametrized mean vector. Uncertainties related to the estimation of the Gaussian residual, on the other hand, can be captured through the covariance matrix estimate [13]

$$\hat{\boldsymbol{\Sigma}} = \frac{1}{n_b - 1}\sum_{k=1}^{n_b} \boldsymbol{\zeta}_k \boldsymbol{\zeta}_k^T, \tag{7}$$

which is calculated as a sample covariance with n_b number of data blocks where $\boldsymbol{\zeta}_k$ is the residual evaluated on each block. The covariance captures the uncertainties in the estimation of the Gaussian residual.

2.4 Predicted Mean Test Response

Statistical hypothesis tests, such as the generalized likelihood ratio (GLR) can be applied for damage detection. The parametrized test statistic is defined as [7]

$$t = \boldsymbol{\zeta}^T \boldsymbol{\Sigma}^{-1} \boldsymbol{\mathcal{J}} \left(\boldsymbol{\mathcal{J}}^T \boldsymbol{\Sigma}^{-1} \boldsymbol{\mathcal{J}} \right)^{-1} \boldsymbol{\mathcal{J}}^T \boldsymbol{\Sigma}^{-1} \boldsymbol{\zeta} \tag{8}$$

and follows a χ^2-distribution with $\nu = \text{rank}(\boldsymbol{F})$ degrees of freedom. The bracketed term in Eq. (8) is known as the Fisher information matrix $\boldsymbol{F} \in \mathbb{R}^{H \times H}$. It can be estimated based on reference data and should be seen as a measure for the detectability of damage with

$$\boldsymbol{F} = \boldsymbol{\mathcal{J}}^T \boldsymbol{\Sigma}^{-1} \boldsymbol{\mathcal{J}}. \tag{9}$$

Assuming that damage can be described through a single parameter change, where all other parameters remain unchanged, the mean test response (i.e. the non-centrality in the χ^2-distribution) can be predicted as [11]

$$\lambda_h = (\Delta\theta_h)^2 F_{hh} f_s T. \tag{10}$$

The damage diagnosis is reliable if the mean test response is sufficiently large, with $\lambda > \lambda_{min}$, because then, the test result is clear despite the uncertainties in the damage-sensitive feature. The minimum mean test response depends on the width of the χ^2-distribution (expressed through the number of degrees of freedom) and can, for example, be determined based on the allowable false-alarm rate and the prescribed probability of detection, which should be close to one-hundred percent [11].

2.5 Hierarchical Parameter Clustering

Damage localization is more challenging than damage detection due to the large number of structural parameters in FE models. Changes in multiple structural parameters have a similar effect on the damage-sensitive residual, and vice versa, it is not possible to identify the structural parameter that has changed. To remedy this, parameters with similar sensitivities are combined to parameter clusters which corresponds to a substructuring of the FE model. To preserve the statistical properties of the damage-sensitive feature throughout the clustering [9], the Jacobian matrix is normalized as follows

$$\tilde{\boldsymbol{\mathcal{J}}} = \boldsymbol{\Sigma}^{-1/2} \boldsymbol{\mathcal{J}}. \tag{11}$$

The first step of the hierarchical clustering approach [16] is to evaluate the similarity of all sensitivity vectors using the dissimilarity measure

$$d_{ij} = 1 - \frac{\tilde{\boldsymbol{\mathcal{J}}}_i^T \tilde{\boldsymbol{\mathcal{J}}}_j}{||\tilde{\boldsymbol{\mathcal{J}}}_i|| \cdot ||\tilde{\boldsymbol{\mathcal{J}}}_j||},$$

where the second term is the cosine between the sensitivity vectors (the columns in the Jacobian matrix). Secondly, the two vectors with the shortest distance are selected. If some of the sensitivity vectors are already clustered, the complete-linkage criterion is applied [17] to evaluate the critical distance D as the one with the maximum distance between individual sensitivity vectors

$$D(C_a, C_b) = \max\{d_{ij} : i \in C_a, j \in C_b\}. \tag{12}$$

The two partitions with the shortest distance D are then combined through averaging, with the cluster centres

$$\mathbf{c}_k = \frac{1}{m_k} \sum_{i \in C_k} \tilde{\boldsymbol{\mathcal{J}}}_i, \tag{13}$$

where m_k is the number of parameters in cluster C_k and $k \in [1, \ldots, K]$ is the number of clusters. The steps from Eq. (12)-(13) are repeated until the distance drops below a user-defined threshold d_{thres}. Ultimately, a clustered Jacobian matrix is obtained

$$\boldsymbol{\mathcal{J}}^c = [\mathbf{c}_1 \ \cdots \ \mathbf{c}_K]. \tag{14}$$

2.6 Damage Localization Test

During damage detection, each structural parameter θ_h is individually tested for changes. In the presented version, the minmax localization test evaluates the minimum likelihood of the tested parameter having changed against the maximum likelihood of changes in untested clusters, as this yields the localization result with the highest localization resolution. Mathematically, this concept is implemented through a geometrical projection as explained in the following. First, the Jacobian matrix is re-organized

$$\boldsymbol{\mathcal{J}}_{h',h'} = [\boldsymbol{\mathcal{J}}_h \boldsymbol{\mathcal{J}}_{\bar{h}}^c], \tag{15}$$

where $\boldsymbol{\mathcal{J}}_h$ is the residual's sensitivity toward the tested parameter from Eq. (5) and $\boldsymbol{\mathcal{J}}_{\bar{h}}^c$ is the untested partition that includes the cluster centres of all parameters from Eq. (14) except the one that contains the tested parameter, so

$$\boldsymbol{\mathcal{J}}_{\bar{h}}^c = \left[\mathbf{c}_1 \ \ldots \ \mathbf{c}_{k(h)-1} \ \mathbf{c}_{k(h)+1} \ \ldots \ \mathbf{c}_K\right].$$

Considering that the clustered Jacobian matrix is already normalized, see Eq. (11), the Fisher information for the reorganized Jacobian matrix can be expressed as

$$\mathbf{F}_{h',h'} = \begin{bmatrix} F_h & \mathbf{F}_{h\bar{h}}^c \\ \mathbf{F}_{\bar{h}h}^c & \mathbf{F}_{\bar{h}\bar{h}}^c \end{bmatrix} = \begin{bmatrix} \boldsymbol{\mathcal{J}}_h^T \boldsymbol{\Sigma}^{-1} \boldsymbol{\mathcal{J}}_h & \tilde{\boldsymbol{\mathcal{J}}}_h^T \tilde{\boldsymbol{\mathcal{J}}}_{\bar{h}}^c \\ \tilde{\boldsymbol{\mathcal{J}}}_{\bar{h}}^{cT} \tilde{\boldsymbol{\mathcal{J}}}_h & \tilde{\boldsymbol{\mathcal{J}}}_{\bar{h}}^{cT} \tilde{\boldsymbol{\mathcal{J}}}_{\bar{h}}^c \end{bmatrix}. \tag{16}$$

Subsequently, the Gaussian residual $\boldsymbol{\zeta}$ is projected onto the tested and untested partitions,

$$\zeta_h = \boldsymbol{\mathcal{J}}_h^T \boldsymbol{\Sigma}^{-1} \boldsymbol{\zeta}, \ \boldsymbol{\zeta}_{\bar{h}}^c = \tilde{\boldsymbol{\mathcal{J}}}_{\bar{h}}^{cT} \boldsymbol{\Sigma}^{-1/2} \boldsymbol{\zeta}, \tag{17}$$

and a geometrical projection is applied to obtain the robust residual and its Fisher information [18]

$$\zeta_h^* = \zeta_h - \boldsymbol{F}_{h\bar{h}}^c \boldsymbol{F}_{\bar{h}\bar{h}}^{c-1} \boldsymbol{\zeta}_{\bar{h}}^c, \tag{18}$$

$$F_h^* = F_h - \boldsymbol{F}_{h\bar{h}}^c \boldsymbol{F}_{\bar{h}\bar{h}}^{c-1} \boldsymbol{F}_{\bar{h}h}^c, \tag{19}$$

respectively. This operation preserves the residual's information content regarding the tested parameter and makes it blind to changes in untested partitions. Ultimately the minmax test statistic is evaluated through

$$t_h^* = \boldsymbol{\zeta}_h^{*T} F_h^{*-1} \boldsymbol{\zeta}_h^*, \tag{20}$$

which is χ^2-distributed with $\nu = 1$ degree of freedom and a mean test response (i.e. a non-centrality) of

$$\lambda_h = \boldsymbol{\delta}_h^T F_h^* \boldsymbol{\delta}_h. \tag{21}$$

The mean test response can be predicted using Eq. (10) after exchanging the Fisher information F_{hh} with the robust Fisher information F_h^* from Eq. (19). Equivalently, the mean test response of a tested but undamaged parameter can be predicted.

2.7 Problem Statement

Stochastic subspace-based damage diagnosis is based on statistical hypothesis tests, such as the general likelihood ratio and the minmax localization test. The tests are data-driven but a FE model is required to physically define

damage, to evaluate the sensitivity towards structural parameter changes, and to localize damage. The model itself is assumed to be perfect and is not updated during the damage diagnosis. FE models are over-parametrized, meaning changes in multiple structural parameters have a similar effect on the damage-sensitive feature. Structural parameters with similar sensitivity vectors have to be combined to parameter clusters, which corresponds to a substructuring of the FE model. The damage localization resolution is a user-defined input parameter and is defined through the cut-off value d_{thres}. It appears intuitive to strive for a high damage localization resolution but the next chapter will show that an increased localization resolution can lead to negative effects, that is, a lower damage detectability and false localization alarms.

3 OPTIMAL DAMAGE LOCALIZATION

This section summarizes an approach from the literature [12] and presents three optimization criteria to find the minimum localizable damage, namely, the damage localization resolution, the minimum detectable damage, and false localization alarms. Moreover, a multi-objective optimization strategy is introduced to find the optimal compromise between the three criteria and to determine the optimum settings for damage localization.

3.1 Damage Localization Resolution

The first criterion is the damage localization resolution. The resolution depends on the number of clusters K because, even though a single parameter change is assumed, undamaged parameters also show a significant test response if they are within the same cluster. A low number of clusters corresponds to a low localization resolution, and a high number of clusters to a high resolution. The higher the resolution, the more accurate the damage localization. Therefore, an objective function can be formed as follows

$$f_1(K) = \frac{K - K_b}{K_g - K_b}, \tag{22}$$

where K is the number of clusters, and g and b indices for a good and bad number of clusters. The normalization through a lower bound $K_b = 2$ and an upper bound $K_g = \text{rank}(F)$ yields in a objective function between zero and one with values close to zero reflecting an ideal localization resolution.

3.2 Minimum Detectable Damage

The second criterion is the minimum detectable damage, that is, the minimum change in local structural design parameters that can reliably be detected based on changes in global damage-sensitive features. It can be calculated based on reference data by rearranging the predictive formula from Eq. (10) for the relative parameter change and substituting the minmax Fisher information from Eq. (19)

$$\Delta_h(K) = \frac{1}{\theta_h^0}\sqrt{\frac{\lambda_{min}}{N \cdot F_h^*}}. \tag{23}$$

The diagnosis is considered "reliable" if the probability of false alarms is low and the probability of detection is high which is equivalent to requiring a minimum mean test response $\lambda = \lambda_{min}$. Equivalently, a damage is "detectable" if it is significant under consideration of typical uncertainties and empirical safety thresholds. The lower the detectable damage, the more sensitive the damage diagnosis. Likewise, the decisive parameter is the one with the highest detectable damage $\Delta_{\max}(K) = \max\{\Delta_1(K), ..., \Delta_H(K)\}$, as this corresponds to the parameter with the lowest damage detectability. An objective function can be formed as follows

$$f_2(K) = \frac{\Delta_{\max}(K) - \Delta_g}{\Delta_b - \Delta_g}, \tag{24}$$

with a lower bound of $\Delta_g = 0\%$ and a upper bound of $\Delta_b = 100\%$.

3.3 False Localization Alarms

The third criterion is the false alarm susceptibility. A false localization alarm is defined as a significant test response for an unchanged parameter that is not within the same cluster as the parameter that has changed due to damage. False alarms occur for inappropriate cluster settings, meaning if the cluster centres are not representative of individual sensitivity vectors or if the sensitivity estimates have not fully converged toward the true value.

The previous section explained how the mean test response could be predicted based on the Fisher information Eq. (10). A reliable damage localization requires that no false localization alarms exceeds the test response for the parameters that have actually changed. Consequently, it is sensible to evaluate the relative test response, using the non-centrality ratio

$$\text{NCR} = \lambda_{h,h'}/\lambda_{h',h'}. \tag{25}$$

The NCR describes the ratio of the predicted mean test response for a tested but unchanged parameter $\lambda_{h,h'}$ to the one of a tested and changed parameter $\lambda_{h',h'}$, cf. Eq. (10) and (19). More details can be found in the literature [12].

Whether or not false localization alarms are significant is determined by introducing a threshold value of, for example, 90%. That means that the NCR must not exceed 90% for any undamaged parameter. To form an optimization criterion the false alarms are evaluated for all possible damage scenarios (i.e. changes in all structural parameters θ_h with $h = 1, \ldots, H$), and the number of scenarios N_{sc} is counted that exhibits false localization alarms. Then, the objective function can then be defined as

$$f_3(K) = \frac{N_{sc}(K) - N_g}{N_b - N_g}, \tag{26}$$

where N_g and N_b are lower and upper bounds that allow the user to weigh the importance of false alarms.

3.4 Pareto Optimization

Finding the minimum localizable damage is a multi-objective optimization problem. It depends on the localization resolution, the minimum detectable damage, and false localization alarms. After scaling with user-defined lower and upper bounds, all three criteria are equally important. For example, a high damage detectability is useless if the localization resolution is low with $K = 1$, because it is merely possible to detect the presence of damage but

not its location. At the same time, a high localization resolution is meaningless if the false localization alarms are excessive, because the actual damage location remains hidden. The localization resolution and the damage detectability are conflicting optimization criteria, meaning it is not possible to improve one criterion without degrading the other.

Dealing with conflicting optimization criteria of equal importance is known as Pareto optimization. The optimal solution is the one that simultaneously optimizes the localization resolution f_1 from Eq.(22), the damage detectability from Eq. (24) and the false alarm susceptibility from Eq. (26). One way to find the optimal solution is to define a compromise function as the Euclidean distance in the three-dimensional optimization space

$$\min_{K} \quad f = \sqrt{f_1(K)^2 + f_2(K)^2 + f_3(K)^2} \qquad (27)$$
$$\text{s.t.} \quad f_1(K) < 1, f_2(K) < 1, f_3(K) < 1.$$

The optimal compromise can then be found by selecting the number of clusters (the localization resolution) with a global minimum in the compromise function f from Eq. (27).

4 NUMERICAL APPLICATION

In this section, the developed methods are applied to the numerical model of a cable-stayed bridge [19]. The goal is to evaluate the optimal substructure arrangement to localize the failure of stay cables and to validate the prediction of the mean test response for damaged and undamaged cables, that is, false localization alarms.

4.1 Model Bridge Description

The specimen is a scaled-down laboratory model of the St. Nazaire cable-stayed bridge in France (scale 1:200), described in [20]. The real bridge and the laboratory model are shown in Fig. 1 and Fig. 2.

Figure 1. St. Nazaire Bridge, Nantes.

The model is split into the main span and two side spans with a length of 2.02 m and 79 cm, respectively. The bridge deck is a steel box girder, continuous over all three spans, with a width of 7.5 cm. The cross-section is composed of foam encased by a trapezoidal steel sheet. The piers at the cable end spans are made of aluminum. The two A-shaped towers, also made of aluminum, rise 33 cm over the steel deck, where the two aluminum posts of each tower are connected at the top through a steel sheet that includes fixtures for stay cables. Each tower sits on top of a monolithic tower pier with two vertical pillars, a transverse

Figure 2. Laboratory model.

beam, and a solid piece that expands to the foundations. The 72 steel cables, connect the upper part of the tower to the deck and form two cable planes in fan-arrangement.

4.2 Finite Element Model

The stochastic subspace-based damage diagnosis method is data-driven, but a FE model is required to parametrize damage and to calculate the sensitivities of the damage-sensitive residual toward structural design parameters. Since the case study in this paper is based on the numerical vibration data, the model is also used for vibration generation.

The FE model from Fig. 3 was created and calibrated by the Department for Civil and Mechanical Engineering in Nantes [20]. It is designed in MATLAB® using custom-code for 3-D beam and truss elements. The continuous deck is discretized into 51 nodes and 50 beam elements with identical cross-sections and material properties over all three spans (Group 1 in Table 1). The piers are split into pier pillars (Group 2) and pier caps (Group 3). The pylons are split into six groups: the piers (Group 4), the V-shaped pier caps (Group 5 and 6), the A-shaped towers (Group 7 and 8), and the vertical cable anchor elements made of metal (Group 9). The stay cables are the only elements that are modelled as trusses (Group 10). In total, the model exhibits 1,038 degrees of freedom. All six degrees of freedom at the two tower foundations and the four pier foundations are fixed, reducing the number of unrestrained degrees of freedom to 1,002.

The model calibration is conducted based on experimental data from the laboratory bridge model from Fig. 2. High uncertainties are expected in the modelling of the bridge deck, because the properties of the epoxy glue and the foam infill are not specified. First, the natural frequencies are extracted using stochastic subspace-based system identification, and subsequently, the cross sectional values of the deck are updated (i.e., the moment of inertia, and the mass density) until a satisfactory match of numerical and experimental frequencies is obtained [20].

The considered natural frequencies and mode shapes of the FE model are summarized in Fig. 4. The mode shape of Mode 2 is similar to Mode 3, but it exhibits no bending components in the towers and a more pronounced longitudinal movement of the deck.

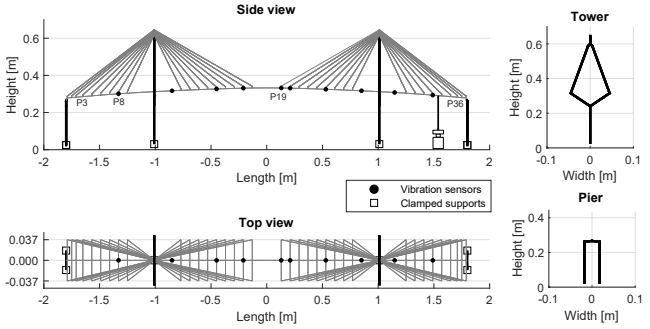

Figure 3. Finite element model in Matlab [19].

No.	ρ $[\frac{kg}{m^3}]$	E $[\frac{MN}{m^2}]$	A $[cm^2]$	I_y $[cm^4]$	I_z $[cm^4]$	J $[cm^4]$
1	37,000	210,000	0.2	2.1	0.18	2.3
2	2,700	69,000	2.0	0.17	0.67	0.83
3	7,800	210,000	2.4	0.8	0.29	1.1
4	2,700	69,000	18	120	6.0	130
5	2,700	69,000	9.0	15	3.0	18
6	2,700	69,000	9.0	15	3.0	18
7	2,700	69,000	0.24	0.0032	0.0072	0.01
8	2,700	69,000	0.24	0.0032	0.0072	0.01
9	7,800	210,000	0.24	0.0032	0.0072	0.01
10	7,800	210,000	77			

Table 1. FE model properties.

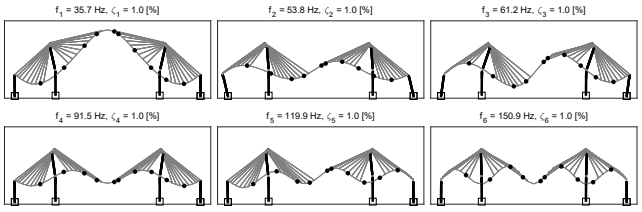

Figure 4. Modes of vibration for damage diagnosis [19].

For vibration generation, the mechanical system matrices are extracted from the model, the modal damping matrix is set up based on an assumed value of 1% critical damping for each mode, and transformed into a state space model in modal coordinates. This allows for the individual modes of vibration to be selected that contribute to the vibration record. Subsequently, a white noise input signal is applied to the vertical degrees of freedom of the deck beam, a transient analysis is run, and the output at the sensor locations from Fig. 3 and 4 is stored after superimposing it with uniformly distributed measurement noise with a magnitude corresponding to 5% of the output variance. All other signal processing parameters are summarized in Table 2.

Signal Processing	
Measurement quantity	acceleration
Sampling frequency	340 Hz
Reference data length	30 min
Training/testing data	30 min

Table 2. Input parameters

a) Damage Parametrization. Damage is defined as a change in the cross-section A of the cables. The same monitoring parameters are assigned to the cables on both sides of the deck, reducing the number of parameters from 72 to 36 with the monitoring vector

$$\boldsymbol{\theta} = [A_1 \ \dots \ A_{36}]\,. \tag{28}$$

The stiffness contribution of three-dimensional truss elements is a linear function of the cross-section A, the modulus of elasticity E, and the cable length L, meaning a change linearization through the Jacobian matrix does not introduce bias.

$$\mathbf{K}_{el}^{loc} = EA/L \begin{bmatrix} 1 & -1 \\ -1 & 1 \end{bmatrix} \tag{29}$$

b) Sensitivity Computation. The Jacobian matrix links changes in the data-driven residual to structural design parameters [9,10]. For its computation, the first six modes of vibration are considered, see Fig. 4. The pole derivatives are computed analytically, and so are the mode shape derivatives. The mode shape derivatives are computed using the modal approach [21], which theoretically requires a loop over all modes of vibration of the FE model. However, the derivatives converge rapidly, and for simplification, only the first 30 modes are considered in this study.

4.3 Optimal Substructures for Damage Localization

Before the optimal substructure arrangement can be found, the main input parameters for the damage diagnosis have to be defined, including the time lag parameters p, q, the system order n, and the number of blocks n_b or the block length $N_b = N_0/n_b$ for the covariance estimation, where $N_0 = Tf_s = 612,000$ is the number of samples from the reference state. For conciseness, all input parameters for the damage diagnosis are summarized in Table 3.

Damage Diagnosis	
Number of channels	r=10
Time lags for Hankel matrix	p/q=4/5
System order for null space	n=12
Block length for covariance	N_b= 10

Table 3. Input parameters

Finding the optimal substructure arrangement is a multi-objective optimization problem. Figure 5 visualizes all three objective functions from Eq. (22), (24), and (26) for a varying number of parameter clusters, together with the compromise function from Eq. (27). The individual objective functions can be interpreted as follows:

- f_1 is the localization resolution (the dashed line). Damage localization with a single parameter cluster is meaningless, so the worst solution with $f_1 = 1$ is achieved for two parameter clusters. With an increasing number of clusters, the localization resolution linearly improves with an optimal value of $f_1 = 0$ for $K_g = \text{rank}(F) = 25$ clusters.
- f_2 is the damage detectability (the solid black line). The detectability is high for a low number of clusters, but for more than six clusters, it gradually worsens with a distinct jump for more than 20 parameter

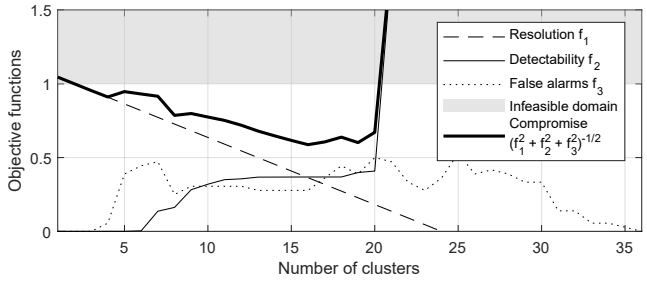

Figure 5. Objective functions.

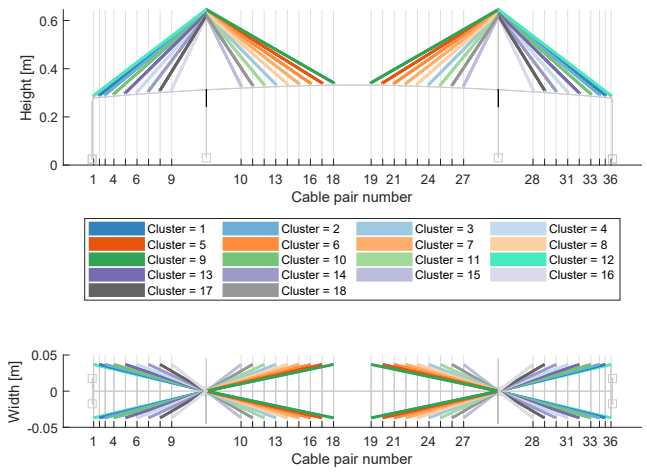

Figure 6. Substructure arrangement.

clusters. This jump indicates that the minimum detectable damage for the parameters with the lowest damage detectability exceeds 100%.

- f_3 is the false alarm susceptibility (the dotted line). False alarms are zero for one or 36 clusters and unequal to zero for most other cases. The solution close to the allegedly optimal point with 20 clusters exhibits a high number of false alarms, which underlines the importance of the false alarm susceptibility as an optimization criterion.

Figure 5 also contains the compromise function (the thick solid black line). It exhibits minima for 16 or 18 parameter clusters, meaning these cluster settings simultaneously maximize the localization resolution and the damage detectability, and minimize false localization alarms. The solution with 18 clusters is visualized in Fig. 6; for this cluster setting, the cable pairs in each cable fan are defined as separate substructures, so the damaged cable pair can be clearly identified. However, due to the symmetry of the bridge, it is not possible to identify the cable fan in which damage has occurred.

4.4 Result Validation

All previous studies in this paper are based on vibration data from the undamaged structure and a FE model. To validate the predictions for the minimum detectable damage from Eq. (23) and the mean test response of undamaged parameters (i.e. the NCR) from Eq. (25), structural damage is now simulated in the FE model by decreasing the cross-sectional area in individual cables pairs by 50%. Since 36 cable pairs are monitored, there are 36 possible damage scenarios, one for each monitoring parameter from Eq. (28).

First, damage scenario P3 is discussed, with a 50% reduction in the cross-section area of cable pair P3. The damage localization results for this scenario is are shown in Figure 7. It appears that the predicted mean test response (plus sign) is close to the measured value (white bar) for the damaged cable pair P3. Cable pair P34 is in the same cluster as cable pair P3, so the test response was to be expected. All other cable pairs are not within the same cluster, but the mean test responses (grey bars) can be predicted with sufficient accuracy. Cable pairs P1, P2, and P4, as well as P33, P35 and P36, exceed the threshold of 90% which is why this scenario is classified as a false alarm scenario.

Secondly, the validation study is repeated for damage scenario P7, P13, and P19, see Figure 7. The predictions appear to be accurate for both changed parameters and unchanged parameters (false localization alarms).

Ultimately, comparing the localization results for the damage scenarios from Figure 7 highlights the importance of all three optimization criteria. Where the localization resolution and the damage detectability are conflicting criteria (meaning it is not possible to improve one without degrading the other), the false alarm susceptibility is not conflicting. Nonetheless, it should be considered as an optimization criterion, because it critically affects the localizability of damage. For example, failure of cable pair P3 leads to significant test responses for three adjacent cable pairs (P1, P2, and P4) and three more on the opposite

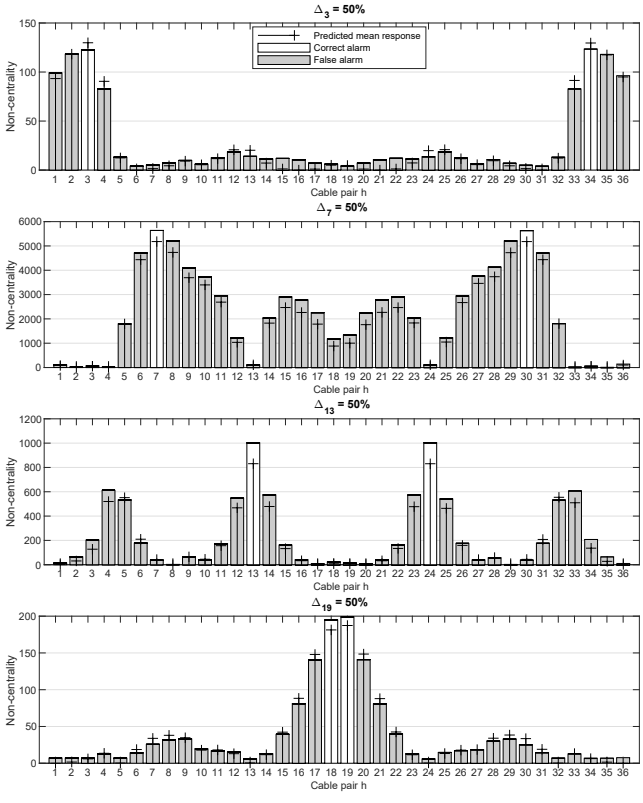

Figure 7. Validating the predictions of the mean test responses for a 50% damage in cable pair P3, P7, P13, P19.

side of the bridge, with NCRs over 95%. Therefore, it cannot be said with certainty whether P2, P3, P34, or P35 is damaged. Scenario P7 is even more ambiguous, as it exhibits test responses for 24 unchanged parameters. With the current settings, both scenarios would be classified as false alarm scenarios. To apply a more severe penalty to scenarios such as P7, the threshold value for the NCR could be lowered from 90% to 50%. On the other hand, damages in cable pair P13 and in P19 can be more clearly localized. To conclude, for a fixed sensors layout, the localizability of some damages is higher than for others, where localizability is a compromise between high damage localization resolution, high detectability, and few false localization alarms.

5 CONCLUSION

This paper describes an approach to determine the minimum localizable damage, which is defined as the minimum damage that can be localized reliably. It presents mathematical formulas to assess the detectability of damage and the false alarm susceptibility. Moreover, it is demonstrated that an increasing damage localization resolution leads to lower damage detectability, and a changing susceptibility for false localization alarms. This paper employs a subspace-based residual vector as a damage-sensitive feature, but the method is readily applicable to any damage-sensitive feature with Gaussian properties.

The analysis is based on vibration data from the undamaged structure and a finite element model. Therefore, the developed method allows the user to evaluate the performance of the damage localization algorithm before damage actually occurs. This is particularly important for unique structures and unprecedented damaged events, where no data is available for different damage scenarios. Being able to evaluate the performance of the damage localization is essential to optimize the sensor layout and to convince decision-makers of the value of implementing a SHM system.

REFERENCES

[1] C. Farrar, K. Worden, Structural health monitoring: A machine learning perspective, Wiley, Oxford, United Kingdom, 2012.

[2] A. Rytter, Vibrational based inspection of civil engineering structures, Ph.D. Thesis, Aalborg University, Aalborg (1993).

[3] R. Brun, P. Reichert, H. R. Künsch, Practical identifiability analysis of large environmental simulation models, Water Resources Research (37) (2001) 1015–1030.

[4] M. Velez-Reyes, G. C. Verghese, Subset selection in identification, and application to speed and parameter estimation for induction machines, in: Proceedings of International Conference on Control Applications, IEEE, Albany, United States, 1995, pp. 991–997.

[5] K. Z. Yao, B. M. Shaw, B. Kou, K. B. McAuley, D. W. Bacon, Modeling Ethylene/Butene Copolymerization with Multi–site Catalysts: Parameter Estimability and Experimental Design, Polymer Reaction Engineering 11 (3) (2003) 563–588.

[6] R. Li, M. A. Henson, M. J. Kurtz, Selection of Model Parameters for Off-Line Parameter Estimation, IEEE Transactions on Control Systems Technology 12 (3) (2004) 402–412.

[7] M. Basseville, M. Abdelghani, A. Benveniste, Subspace-based fault detection algorithms for vibration monitoring, Automatica 36 (1) (2000) 101–109.

[8] M. Basseville, L. Mevel, M. Goursat, Statistical model-based damage detection and localization: Subspace-based residuals and damage-to-noise sensitivity ratios, Journal of Sound and Vibration 275 (3-5) (2004) 769–794.

[9] É. Balmès, M. Basseville, L. Mevel, H. Nasser, W. Zhou, Statistical model-based damage localization: A combined subspace-based and substructuring approach, Structural Control and Health Monitoring 15 (6) (2008) 857–875.

[10] S. Allahdadian, M. Döhler, C. Ventura, L. Mevel, Towards robust statistical damage localization via model-based sensitivity clustering, Mechanical Systems and Signal Processing 134 (2019) 106341.

[11] A. Mendler, M. Döhler, C. E. Ventura, A reliability-based approach to determine the minimum dectable damage for statistical damage detection, Mechanical Systems and Signal Processing (under review) (2021).

[12] A. Mendler, M. Döhler, C. Ventura, L. Mevel, Clustering of Redundant Parameters for Fault Isolation with Gaussian Residuals, in: Proceedings of the IFAC - 21st World Congress of the International Federation of Automatic Control, Berlin, Germany, 2020.

[13] A. Benveniste, M. Basseville, G. Moustakides, The asymptotic local approach to change detection and model validation, IEEE Transactions on Automatic Control 32 (7) (1987) 583–592.

[14] P. van Overschee, B. de Moor, Subspace identification for linear systems: Theory, Implementation, Application, Kluwer Academic Publishers, Boston/London/Dordrecht, 1995.

[15] B. Peeters, G. De Roeck, Reference-based stochastic subspace identification for output-only analysis, Mechanical Systems and Signal Processing 13 (6) (1999) 855–878.

[16] S. Allahdadian, M. Döhler, C. Ventura, L. Mevel, Towards robust statistical damage localization via model-based sensitivity clustering, Mechanical Systems and Signal Processing 134 (2019) 106341.

[17] R. O. Duda, P. E. Hart, D. G. Stork, Pattern classification, John Wiley & Sons, New York, United States, 2012.

[18] M. Döhler, L. Mevel, Q. Zhang, Fault detection, isolation and quantification from Gaussian residuals with application to structural damage diagnosis, Annual Reviews in Control 42 (2016) 244–256.

[19] A. Mendler, Minimum diagnosable damage and optimal sensor placement for structural health monitoring, Ph.D. thesis, University of British Columbia, Vancouver, Canada (2020).

[20] A. Cadoret, C. Freyssinet, Y. Lecieux, Fault detection using modal analysis (in French), Tech. rep., University of Nantes, Nantes (2020).

[21] T. R. Sutter, C. J. Camarda, J. L. Walsh, H. M. Adelman, Comparison of several methods for calculating vibration mode shape derivatives, AIAA journal 26 (12) (1988) 1506–1511.